Journal of Engineering Science and Technology
Vol. 17, No. 1 (2022) 0508 - 0522

CRACKED SOIL BEHAVIOUR TREATED WITH GEOPOLYMER FOR RIVER EMBANKMENT USING A FUZZY C-MEANS METHOD

YERRY K. FIRMANSYAH[1,3,*], RIA A. A. SOEMITRO[1], DWA D. WARNANA[2], JANUARTI J. EKAPUTRI[1]

[1]Civil Engineering Department, Faculty of Civil, Planning and Geo Engineering, Institut Teknologi Sepuluh Nopember, Indonesia, Jl. Raya ITS, Keputih, Surabaya, East Java, Indonesia
[2]Geophysical Engineering Department, Faculty of Civil, Planning and Geo Engineering, Institut Teknologi Sepuluh Nopember, Indonesia, Jl. Raya ITS, Keputih, Surabaya, East Java, Indonesia
[3]Civil Engineering Department, Faculty of Engineering, Universitas Pembangunan Nasional "Veteran" Jawa Timur, Indonesia, Jl. Raya Rungkut Madya, Gunung Anyar, Surabaya, East Java, Indonesia
*Corresponding Authors: yerry@ce.its.ac.id

Abstract

Bengawan Solo, alternatively Solo River, is listed as one of Indonesia longest rivers. In river embankments, failures often occur due to fluctuations in river water levels and climate change. Cracked soil is one of the triggers to accelerate soil saturation. Therefore, improving the soil properties of the river embankments must be carried out. Furthermore, the change of soil properties is continued due to the cycle of drying process. One of the efforts to improve soil properties is by the chemical treated soil e.g., geopolymerization. Geopolymer treated soil still has expansive characterization since the soil physical properties easily change during drying process. The composition of the geopolymer used consists of fly ash and alkali activators. MATLAB software using Fuzzy C-Means (FCM) method was operated to determine the crack intensity of cracked soil obtained from laboratory tests. The analysis results in form of image displayed that the crack patterns showing geometric features were affected by the drying process with 10% intervals of content of water decrease up to the air-drying condition was accomplished. One of the research results that have been obtained on stabilized soil and without stabilization of FAG (Fly Ash based Geopolymer) that the Crack Intensity Factor (CIF) value of 10% FAG material as stabilization was 0.99 %. Next, CIF value of soil without material stabilization was 1.16%. It was found out that the geopolymer application has been used successfully as a stabilizing material in the Bengawan Solo River embankment.

Keywords: Cracked soil, Drying condition, Fuzzy C-Means (FCM), Geopolymer, River embankment.

1. Introduction

As the longest river in Java Island, Bengawan Solo, an approximately 600 km in length, is precisely located in Central Java with its river flows to East Java, to be exactly in sea north of Surabaya [1], as shown in Fig. 1. The overtopping and failure of the embankments alongside the Bengawan Solo have its own history [2, 3]. The most population live across the river basin of Solo River reaching 810 people/km, in other words, the population around the river live straight to the flood embankments, thus relocation or fatalities can occur due to flooding [2].

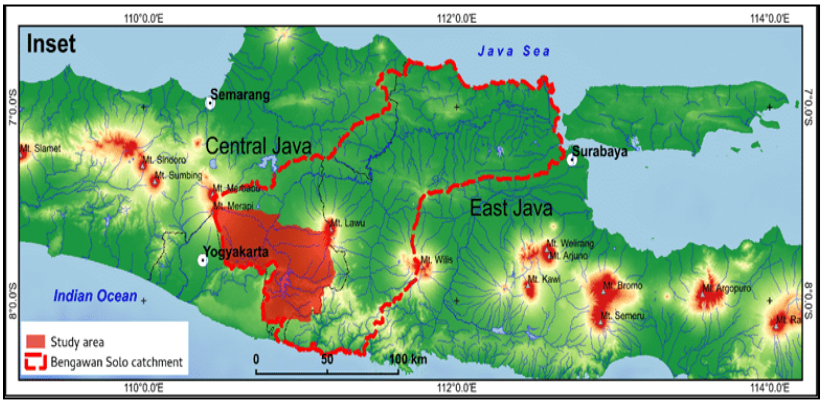

(a)

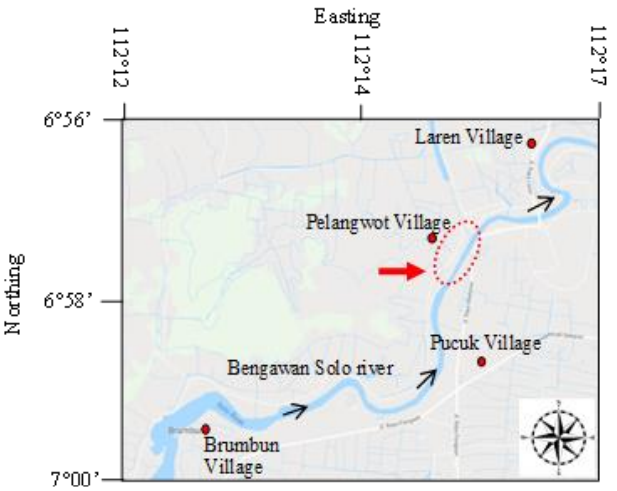

(b)

Fig. 1. Map of Bengawan Solo (a) catchment area in East Java, Indonesia [4]; (b) Site located in Pelangwot [5].

If additives are put on reactive soil to prompt long-term strength development using pozzolanic reaction, it will generate soil stabilization. Widely used in soil improvement, there are various stabilization additives that can be found. In this

study Fly ash was used as a stabilization material because this material is a waste in Indonesia so that it has very abundant material availability.

To mention some of them are lime, cement, fly ash, slag, and so on [6]. To stabilize soil, Geopolymer is one of a sufficient and potential materials. This material is made from aluminosilicate that is mixed with alkali-activator using natural reactive property [7]. As new materials of cementitious, geopolymers have three-dimension structure of alumina silicate gel which is materialized through low temperature chemical activation of solid aluminosilicate comprising precursor materials [8]. Numerous alumina silicate can be found in precursors that are applied in geopolymer synthesis [9, 10], for instance is fly ash which displays features of higher purity as well as higher reactivity than other materials and has proven to have high strength [11, 12] and low permeability geopolymers [13].

In many studies, fly ash is used to produce geopolymers that will be used as construction materials. Fly ash can be generated from precipitation of electrostatic using coal combustion products. Fly ashes had been produced for more than 500 million tons annually by petrochemical industries and power stations in the world, yet only 20-30% of those mass production is used mostly by industries producing cement or concrete as the filler or supplementary material for cementitious [14]. Thus, it is worth to note that fly ash has potential in economic and environmental aspects for synthetizing geopolymer. Nevertheless, as its feature of high reactivity cannot be found in all fly ashes [15], the mixture of this material and geopolymer precursors is inevitable to produce strong materials and rate of microstructural development.

To control soil in drying condition, it is essential to consider soil's compactedness and volumetric shrinkage as mechanical and physical parameters [1, 16-18]. Image processing was employed to observe the drying process effect on the crack patterns geometric characteristics [16, 19, 20]. The previous researches imply that, quantitatively, image processing may be performed to find the cracking behavior, which is the drying process dependence [19].

Cracked soil images obtained from tests of laboratory may be used to discover the intensity of cracking by Fuzzy c-means numerical modeling. This modeling is method has been performed on feature analysis, classifier designs and clustering successfully in the practice of geology, astronomy, target recognition, image segmentation, and medical imaging [21-25]. This research was done to distinguish the feature of cracked soil specifically to index the Crack Intensity Factor or CIF through FCM method. Crack Intensity Factor or CIF is the comparison of the surface cracking area to the total of the sample's surface area.

2. Constituents of Geopolymer Material

2.1. Geopolymers

Two primary elements are involved in geopolymers: alkaline liquid source materials. Geopolymers' main materials, which are alumina-silicate-based, should comprise aluminum (Al) and silicon (Si) in abundant amount. The geopolymer's source materials may contain natural minerals, for instance clays, kaolinite, etc. The source material for by-product may contain, for example, silica fume, fly ash, rice husk ash, red mud, slag. The option of geopolymer's source materials lies on several factors, for example cost, availability, application types, and specific demand of the direct users [26]. Poly (sialate) is polymer with chain and circular

form comprising Si4+ and Al3+ in IV-fold coordinated with oxygen and the character differs from amorphous to semi-crystalline [27]. Several frameworks can be seen in the following Fig. 2.

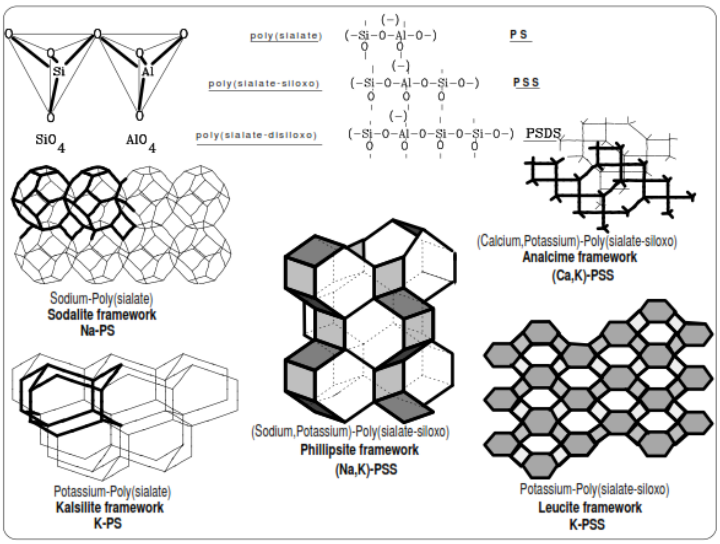

Fig. 2. Computerized graphics of polymer molecule Mn–(Si-O-Al-O-)n poly(sialate) and Mn–(Si-O-Al-O-Si-O-)n poly(sialate-siloxo), and other frameworks [27].

2.2. Fly ash (FA)

Based on the terminology of American Concrete Institute (ACI) Committee 116R, the definition of fly ash is 'the finely divided residue that results from the combustion of ground or powdered coal and that is transported by flue gases from the combustion zone to the particle removal system' (ACI Committee, 2004). The separation of fly ash from the combustion gases by system of dust collection is conducted whether through mechanical or through electrostatic precipitators prior to gas releasing to the air. The shape of fly ash particles can be spherical and thinner compared to Portland cement and lime particles. The diameter ranges from <1 μm to ≤ 150 μm [26-28], as shown in Fig. 3. It shows the SEM of fly ash; (a) Ungraded fly-ash and (b) Graded fly-ash.

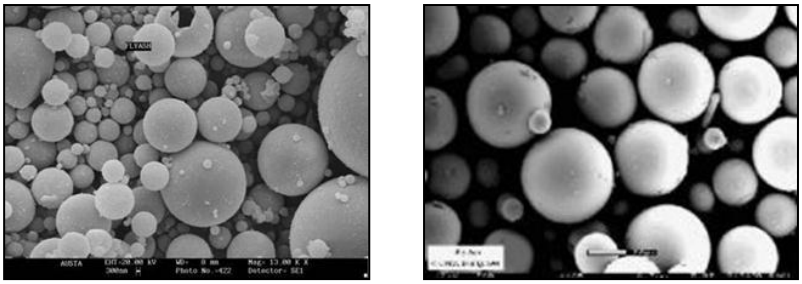

(a) **(b)**

Fig. 3. SEM of fly ash (a) Ungraded fly-ash (b). Graded fly-ash [26].

Composition of chemical consists of aluminium (Al_2O_3), silicon oxides (SiO_2), calcium (CaO), and iron (Fe_2O_3). Meanwhile in smaller amount, there are also found potassium, magnesium, sodium, sulphate, and titanium. Some of the noticeable features of fly ash are fineness, loss on ignition (LOI), and uniformity. Fineness feature majorly lies on the condition of operation of the coal grinding process and coal crushers. LOI determines the carbon residue in the ash that cannot be burned. More reactive ash containing less carbon might be resulted from finer gradation [26].

FA in this study was obtained from Tanjung Jati 3-4, local Indonesian supplier. Table 1 describes composition of chemical in FA employing X-ray fluorescence (XRF). The amount of the main items of FA (Al_2O_3, Fe_2O_3, SiO_2) is 82.0 %, whereas the amount of CaO is 8.0%. Thus, this composition falls into Class F FA. Classification of fly ash is generally carried out by considering the levels of chemical compounds (SiO_2 + Al_2O_3 + Fe_2O_3), CaO levels (high calcium and low calcium), and carbon levels (high carbon and low carbon). Type F fly ash is fly ash made ASTM C618-19 [29].

Table 1. Chemical properties of FA.

Chemical composition (%)	SiO_2	Fe_2O_3	Al_2O_3	CaO	MoO_3	K_2O	Na_2O
Concentration (%)	43.60	23.00	15.40	8.00	3.32	2.48	N.D

2.3. Alkaline activators

Alkaline activators commonly used in geo-polymerization is the mixture between sodium silicate or potassium silicate and sodium hydroxide (NaOH) or potassium hydroxide (KOH) [30, 31]. According to Palomo et al. [30], alkaline liquid type has a significant role during the process of polymerization. If the alkaline liquid comprises silicate that is soluble, whether it contains potassium silicate or sodium, the reactions will happen at a high rate, in contrast to process with the alkaline hydroxides alone. As affirmed by Xu and van Deventer (2001) [9], if sodium silicate is added into sodium hydroxide as the alkaline liquid, it will increase the chemical process of the solution and source material. Moreover, following the research on geo-polymerization of sixteen natural minerals of Al-Si, it was discovered that NaOH provoked greater chance of mineral separation compared to KOH solution. The mixture of Na_2SiO_3, containing of 36.40% SiO_2 and 18.50% Na_2O by weight, and NaOH 4 M.

3. Materials and Methods

3.1. Soil

The examined soil specimen is the embankment across Bengawan Solo at Pelangwot Village, Bojonegoro Regency, Indonesia, Fig. 1(b). The specimens were taken from 0.3 m to 0.5 m in depth from the surface, both disturbed and undisturbed samples. The classification of soil obtained is inorganic silt with high compressibility [17]. The following Table 2 shows several basic soil properties and the soil chemical composition by X-Ray Fluorescence method is presented in Table 3. It shows the results that the main chemical compositions consist of Calcium (Ca) and Silica (Si). Clay fraction's minerals is an essential part in the soil properties, for instance, features of strength and plasticity [17].

Table 2. Properties of Bengawan Solo soil [5].

Properties	Value (%)
Liquid limit	135.00
Plastic limit	100.80
Plasticity index	34.20
Linear shrinkage	9.90
Volumetric shrinkage	12.55
Particle Size Distribution (PSD)	
Sand	4.54
Silt	44.98
Clay	50.48

Table 3. The chemical composition of Bengawan Solo river embankment soil [5].

Compound	SiO_2	Fe_2O_3	CaO	Al_2O_3	K_2O	TiO_2	MnO
Concentration (%)	40.30	25.20	18.40	12.00	1.10	2.02	0.58

To study cracked soil behaviour, first, the soil was air-dried and sieved through a 4.75 mm sieve, and the soil specimen was remoulded on a circular plate with 1 cm soil thickness and 10 cm surface diameter (Fig. 4). The sieved soil was mixed with water to achieve optimum moisture content and soil density concerning the compaction test. The sample has been prepared manually placing soil into the moulds. The sample has been measured and recorded the weight of the specimen with water content decreasing at 10% intervals until air-dried conditions were achieved.

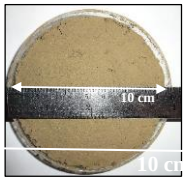

Fig. 4. Soil specimen was remoulded on a circular plate with 1 cm soil thickness and 10 cm surface diameter.

3.2. Various molarity of NaOH

Rangan [32] recommends mixing both solutions at least a day before use for the liquid of alkaline. It is also recommended to apply the sodium silicate solution A53 use with a SiO_2 -to- Na_2O ratio by mass of about two and sodium hydroxide with purity of 97-98%. The sodium hydroxide solution concentration that can be utilized is range from 4 to 8 M.

In this study, it is revealed that the solution of 4 M NaOH contributes to the medium compressive strength and not brittle when the process of soil mixing. Nevertheless, other studies discovered that increasing the molarity of NaOH can increase the compressive geopolymer strength [33]. Based on that finding, when the activator concentration is above a solution of 10 M NaOH, a polymer formation lower rate is formed because of the high NaOH concentration, causing a decreased strength [34].

3.3. Various fly ash/alkaline activator mass ratios and Na_2SiO_3 /NaOH mass ratios

Previous studies [33, 35] found that the compressive strength increases as the activator solution and fly ash content increase. Several studies [30, 36] confirmed that

a geopolymer with a fly ash/L 3.3-4.0 ratio can be utilized. Nonetheless, other studies [30] clarified that the ratio of fly ash/alkaline activator cannot be a relevant parameter affecting the compressive strength. This finding is disputed by other studies. Rattanasak and Chindaprasirt [37] concluded that the mass ratio use of Na_2SiO_3 to NaOH of 1.0 contributes to up to 70 MPa strength. Hardjito et al. [33] even revealed that the use of Na_2SiO_3/NaOH with a 2.5 ratio contributes to the highest compressive strength compared to the use of Na_2SiO_3/NaOH with a 0.4 ratio. Sathonawaphak et al. [38] further stated that a geopolymer with a fly ash/alkaline activator 1.4-2.3 ratio resulted in a 42-52 MPa high compressive strength. Further, their study found that 1.5 became the optimum Na_2SiO_3/NaOH ratio and the maximum strength was 48 MPa. However, in this study, the effective composition was obtained at the 1.86 fly ash/alkaline activator ratio and 1.6 Na_2SiO_3/NaOH ratio.

3.4. Fly ash based geopolymer (FAG) stabilized soil embankment

The FA based geopolymer content was various at 10%, 20%, 30%, and 40% by dry soil weight and the ratio of the Na_2SiO /NaOH, the concentration of NaOH, ratio of alkaline activator/FA, and water content were fixed at the optimal ingredient because of the FA geopolymer stabilized soil test. After all materials were well mixed, specimens were tested for compaction.

3.5. Image processing

Digital image processing techniques are frequently applied in analysing the crack pattern structure. Figure demonstrated the digital image processing procedure. First, a grey level image, Fig. 5(a), changed to the crack pattern colour photograph; second, the contrast in grey level between aggregates and cracks was sufficiently high, hence, the grey level image can be segmented into aggregates and cracks utilizing a simple grey threshold [39]. This process was termed binarization, causing the binary white and black image, Fig. 5(b). It is shown that the white areas denote the aggregates, and the black areas denote the crack networks; third, schematized crack network structure was formed by skeletonizing in determining the lengths and crack intersections, Fig. 5(c) [40], this operation applied the medial axis transformation (MAT) method [41]. All the processes could be operated conveniently and automatically in the software MATLAB based FCM.

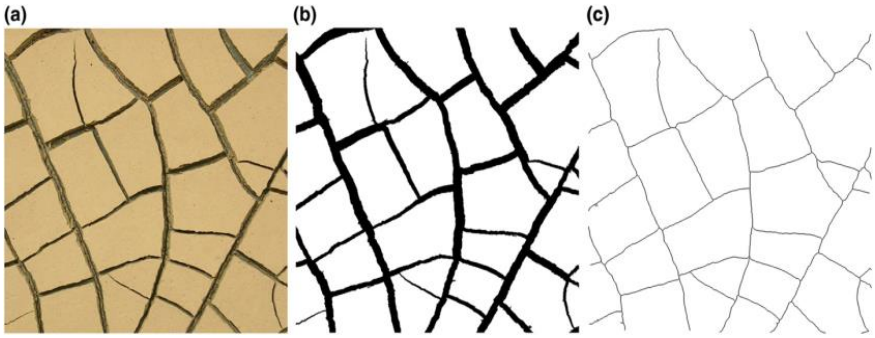

Fig. 5. Digital image processing procedure. (a) Initial grey level image, (b) binary white and black image, and (c) crack network skeleton [40].

3.6. Fuzzy C-means (FCM) clustering

The FCM algorithm assigns pixels to each category by using fuzzy memberships. Let X = (x_1, x_2,...,x_N) denotes an image with N pixels to be partitioned into c clusters, where is represents multispectral (features) data [5, 24]. The algorithm is an iterative optimization that minimizes the cost function defined as follows:

$$J = \sum_{j=1}^{N} \sum_{i=1}^{c} u_{ij}^{m} \left\| x_j - v_i \right\| \quad (1)$$

where u_{ij} represents the membership of pixel x_j in the i th cluster, v_i is the i th cluster centre, $\|.\|$ is a norm metric, and m is a constant. The parameter m controls the fuzziness of the resulting partition, and $m = 2$ is used in this study.

The cost function is minimized when pixels close to the centroid of their clusters are assigned high membership values, and low membership values are assigned to pixels with data far from the centroid. The membership function represents the probability that a pixel belongs to a specific cluster. In the FCM algorithm, the probability is dependent solely on the distance between the pixel and each individual cluster centre in the feature domain [5, 24]. The membership functions and cluster centres are updated by the following:

$$u_{ij} = \frac{1}{\sum_{k=1}^{c} \left(\frac{\left\| x_j - v_i \right\|}{\left\| x_j - v_k \right\|} \right)^{2/(m-1)}}, \quad (2)$$

and

$$v_i = \frac{\sum_{j=1}^{N} u_{ij}^{m} x_j}{\sum_{j=1}^{N} u_{ij}^{m}}. \quad (3)$$

Starting with an initial guess for each cluster centre, the FCM converges to a solution for v_i representing the local minimum or a saddle point of the cost function. Convergence can be detected by comparing the changes in the membership function or the cluster centre at two successive iteration steps.

4. Findings and Discussion

4.1. Compaction test

The specimen of soil was arranged as Proctor compacted. To investigate the Bengawan Solo River embankment compaction behaviour was important, as the soils were to be compacted and remoulded for tests of the laboratory, and the compaction test guide results in the sample of remoulded crack soil. The methods of a standard test for laboratory compaction utilizing soil characteristics using standard effort were conducted based on The American Society for Testing Materials (ASTM) D698, with 12,400 ft-lbf/ft^3 input energies per unit volume.

The value of the dry density on the test specimens increased along with the addition of FAG material. Figure 6 demonstrates the compaction test results with variations in the fly ash based geopolymer percentage.

The addition of FAG material by 10%, 20%, and 30% show a dry density value not greater than the initial soil condition. However, adding FAG by 40% significantly increases the dry density value. The dry density value will decrease if the water content is more than 18.4%. This shows that the effect of water has an

influence on the density test. The increase in dry density in this case is due to a chemical reaction between the alkaline activator, fly ash, and soil so that a very strong aggregate bond occurs. In this phenomenon there is a change in the decreasing of specific gravity and increasing the void ratio. The optimum moisture content (OMC) has the same characteristics for initial soil and the addition of FAG by 10%, 20%, and 30% which is around 25% to 27.5%.

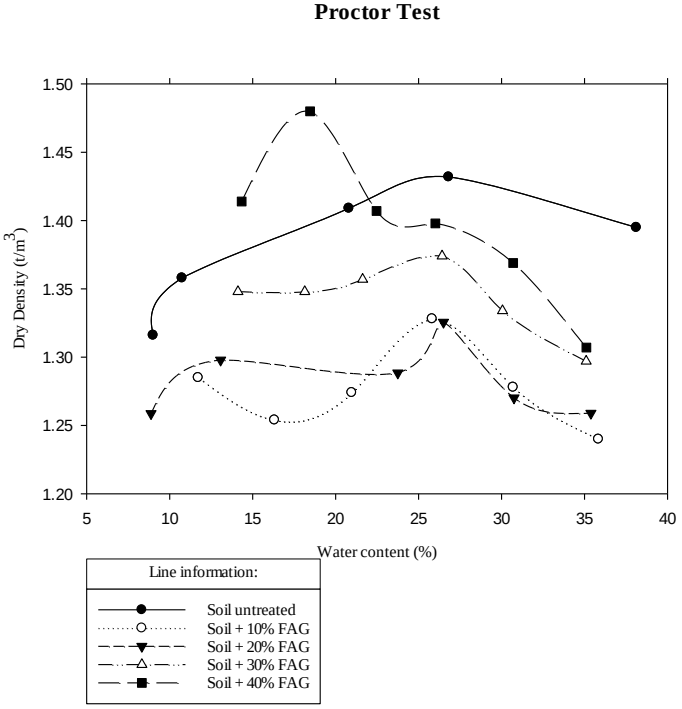

Fig. 6. The results of compaction tests with variations in the percentage of FAG.

The addition of FAG materials by 10%, 20%, and 30% indicates that the dry density value is not greater than the initial soil condition because the specific gravity value of the fly ash material is smaller than the soil even though there has been a bond between the granules due to the presence of alkali activators. While at a FAG percentage 40% produces a bond between fly ash and alkali activators making a perfect bond so that the specific gravity value is greater than the initial soil.

4.2. FAG concentration level

In this section, the analysis focuses on the level of chemical concentration in soil material that is stabilized with FAG. Chemical concentration analysis using a micro-XRF spectrometer with a total number of pixels of 555,800 pixels. The material tested was soil stabilized with FAG and initial soil, as shown in Fig. 7. The evaluation of chemical concentration is focused on the elements that dominate in FAG and soil materials such as Si, Al, Ca, and Fe. The concentration level results of the chemical elements, as shown in Fig. 8 and Table 4.

(a) **(b)**

Fig. 7. Material test preparation for (a). Soil + FAG, and (b). Initial soil.

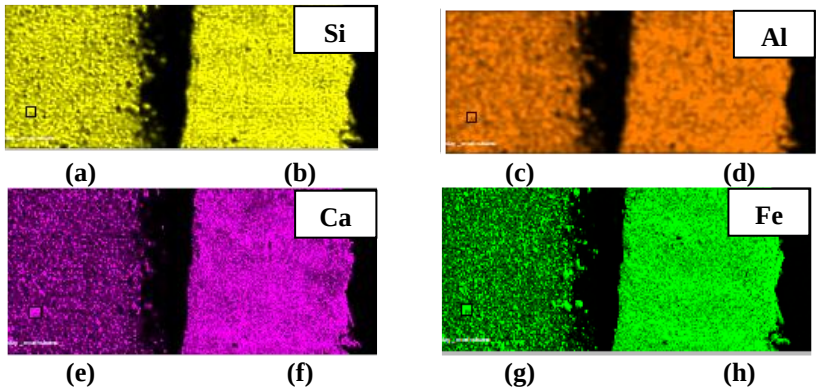

Fig. 8. Chemical elements concentration of (a). Si in Soil + FAG; (b). Si in Initial soil; (c). Al in Soil + FAG; (d). Al in Initial soil; (e). Ca in Soil + FAG; (f). Ca in Initial soil; (g). Fe in Soil + FAG; (h). Fe in Initial soil.

Table 4. The chemical composition using micro-XRF spectrometer.

Element	Soil + FAG (%)	Initial Soil (%)
Si	27.11	24.41
Al	11.30	10.22
Ca	6.63	8.36
Fe	6.01	9.43

Based on Table 4, it can be seen that there is a change in the value of each element. For Si and Al parameters in the soil tends to increase after the presence of FAG material. Meanwhile, Ca and Fe parameters in the soil tend to decrease after being mixed with FAG. Fernández-Jiménez and Palomo [42] and Rees et al. [43] examined the mechanism of geopolymerization during the NaOH fly ash activation by methods of SEM/TEM and ATR-FTIR respectively [44]. The reaction was started with the Al and Si dissolution from particles of the precursor into the solution of alkaline, then followed by the polymerization (including nucleation)

into an "Al-rich" phase of initial gel that is later gradually converted into a more Si-rich final gel of geopolymer.

4.3. Quantitative analysis of crack intensity

By implementing the method of FCM, this study aims at observing cracked soil mostly to index the Crack Intensity Factor (CIF) on the soil. This method indicates a highly precise accuracy level, yet the picture resolution is needed to be clear. The method of FCM was implemented to investigate the digital images for crack deformation and evolution. Whereas the visual analysis in examining the crack soil used the FCM method of MATLAB software-based [5]. The spaces of various features can represent an image, and the image categorized the algorithm of FCM by classifying points of similar data in the feature space into the clusters. The clustering can be accomplished by iteratively minimizing a function of the cost that is dependent on the pixels of distance to the cluster centres in the feature domain. The technique of a custom application is applying the Crack Identification of Soil (CIS). Crack Identification of Soil software was created to quantify and characterize cracks of soil. Then, the FCM method of MATLAB software analysed and calculated the results as demonstrated in Fig. 9. The purple colour shown in Fig. 9 is the result of a crack detected from the MATLAB software based FCM method.

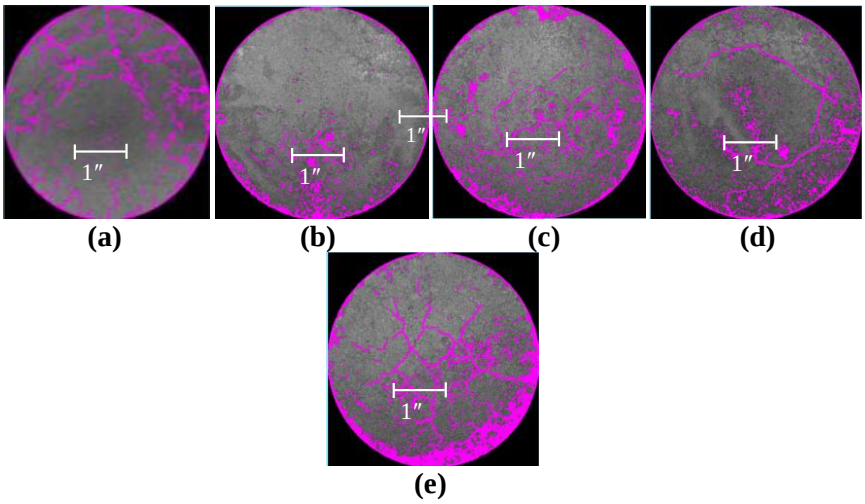

Fig. 9. Crack detected for (a). Initial soil; (b). Soil + 10% FAG; (c). Soil + 20% FAG; (d). Soil + 30% FAG; (e). Soil + 40% FAG.

The CIF (Crack Intensity Factor) is the surface crack area ratio to the entire surface soil area. Thus, the greater CIF value indicates that more cracks occur in percent. The results of the investigation into the presence of FAG material as much as 10%, 20%, 30%, and 40% are mixed with soil embankment from the Bengawan Solo River. It shows that the greater of FAG material used, the CIF value increases. The most significant increase in CIF when using 40% FAG material, as shown in Fig. 10. The result of CIF. The ideal condition for using FAG as a soil stabilization material, especially in preventing cracking in surface areas is 10% FAG.

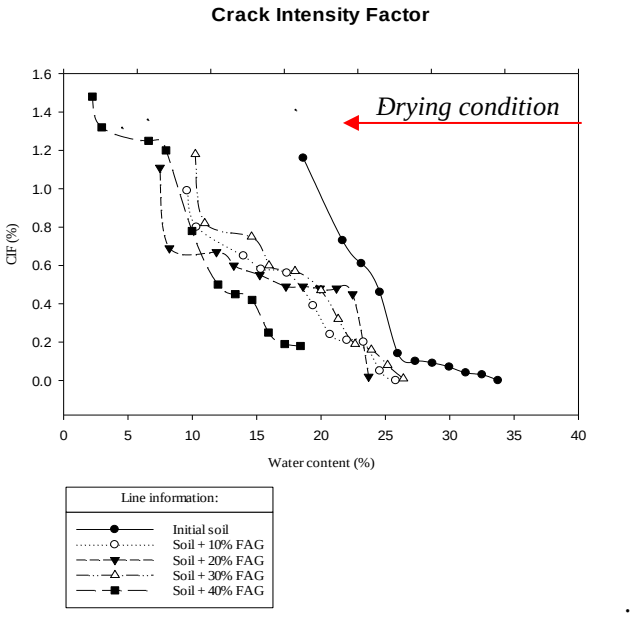

Fig. 10. The result of crack intensity factor (CIF).

5. Conclusions

An investigation has been conducted on the use of FAG as a soil stabilization material with FAG variation is 10%, 20%, 30%, and 40%. Furthermore, the analysis uses the FCM method, and several conclusive observations are obtained as follows:

- The proctor test analysis results show that the more FAG material is used, the dry density increases.
- Whereas the CIF value is the opposite of the proctor test phenomenon. That is, the greater of FAG percentage material substituted on soil makes higher the CIF value.
- The ideal use of FAG material is 10%, especially for the Bengawan Solo River embankment area in the Pelangwot section because it has the smallest CIF value.
- The cracked soils calculation and identification by using FCM (Fuzzy C-Means) were categorized as successful and cracked soils happened in the first step process of drying.

Acknowledgments

We would like to express our gratitude to The Indonesian Ministry of Research, Technology, and Higher Education, especially for the program of PMDSU (Pendidikan Magister Doktor Sarjana Unggul) and UPN "Veteran" Jatim for providing us scholarship and also research grant to complete this research.

Abbreviations

ACI	American Concrete Institute
ASTM	The American Society for Testing Materials
ATR	Attenuated Total Reflection
CIF	Crack Intensity Factor, %

CIS	Crack Identification of Soil
FA	Fly Ash
FAG	Fly Ash based Geopolymer
FCM	Fuzzy C-Means
L	Liquid alkaline activator
LOI	Loss On Ignition
MAT	Medial Axis Transformation
MATLAB	Programming language developed by MathWorks
OMC	Optimum Moisture Content
PMDSU	Pendidikan Magister Doktor Sarjana Unggul
SEM	Scanning Electron Microscopy
TEM	Transmission Electron Microscopy
UPN	Universitas Pembangunan Nasional
XRF	X-ray Fluorescence

References

1. Mountassir, G.E.; Sanchez, M.; Romero, E.; and Soemitro, R.A.A. (2010). Behaviour of compacted silt used to construct flood embankment. *Proceedings of the Institution of Civil Engineers-Geotechnical Engineering*, 164(3), 195-210.
2. Hidayat, F.; Sungguh, H.M.; and Harianto. (2008). Impact of climate change on floods in Bengawan Solo and Brantas river basins, Indonesia. *Proceedings of the* 11*th International Riversymposium*, Brisbane.
3. The Jakarta Post (2009). Bojonegoro levee section collapses, affected residents flee. Retrieved 28 February 2009, from http:// www.the jakartapost.com/news/ 2009/02/28/bojonegoro-leveesection-collapses-affected-residents-flee.html.
4. Rustanto, A.; Booij, M.J.; Wösten, H.; and Hoekstra, A.Y. (2017). Application and recalibration of soil water retention pedotransfer functions in a tropical upstream catchment: Case study in Bengawan Solo, Indonesia. *Journal of Hydrology and Hydromechanics*, 65(3), 307-320.
5. Firmansyah, Y.K.; Soemitro, R.A.A.; Warnana, D.D.; and Ekaputri, J.J. (2019). Cracked soils behavior due to drying conditions using a Fuzzy C-Means method. *International Journal of GEOMATE*, 17(64), 209-216.
6. Kavak, A.; and Bilgen, G. (2016). Reuse of ground granulated blast furnace slag (GGBFS) in lime stabilized embankment materials. *IACSIT International Journal of Engineering and Technology*, 8(1), 11-14.
7. Dungca, J.R.; Ang, K.D.; Isaac, A.M.L.; Joven, J.J.R.; and Sollano, M.B.T. (2019). Use of dry mixing method in fly ash based geopolymer as a stabilizer for dredged soil. *International Journal of GEOMATE*, 16(57), 9-14.
8. Deventer, J.S.J.; Provis, J.L.; and Duxson, P. (2012). Technical and commercial progress in the adoption of geopolymer cement. *Minerals Engineering*, 29, 89-104.
9. Xu, H.; and Deventer, J.S.J. (2001). Effect of alkali metals on the preferential geopolymerization of stilbite/kaolinite mixtures. *Industrial and Engineering Chemistry Research*, 40(17), 3749-3756.
10. Andini, S.; Cioffi, R.; Colangelo, F.; Grieco, T.; Montagnaro, F.; and Santoro, L. (2008). Coal fly ash as raw material for the manufacture of geopolymer-based products. *Waste Management*, 28(2), 416-423.

11. Duxson, P.; Provis, J.L.; Lukey, G.C.; Mallicoat, S.W.; Kriven, W.M.; and Deventer, J.S.J. (2005). Understanding the relationship between geopolymer composition, microstructure and mechanical properties. *Colloids Surfaces A*: *Physicochemical and Engineering Aspects*, 269(1-3), 47-58.
12. Zhang, Z.; Wang, H.; Zhu, Y.; Reid, A.; Provis, J.L.; and Bullen, F. (2014). Using fly ash to partially substitute metakaolin in geopolymer synthesis. *Applied Clay Science*, 88-89, 194-201.
13. Zhang, Z.; Yao, X.; and Zhu, H. (2010). Potential application of geopolymers as protection coatings for marine concrete. I. Basic properties. *Applied Clay Science*, 49, 1-6.
14. Ahmaruzzaman, M. (2010). A review on the utilization of fly ash. *Progress in Energy and Combustion Science*, 36(3), 327-363.
15. Duxson, P.; and Provis, J.L. (2008). Designing precursors for geopolymer cements. *Journal of the American Ceramic Society*, 91(12), 3864-3869.
16. Atique, A.; and Sanchez, M. (2011). Analysis of cracking behavior of drying soil. *Proceedings of the* 2*nd International Conference on Environmental Science and Technology*. Singapore, 66-70.
17. McCloskey, G.; Sanchez, M.; and Dyer, M. (2008). Experimental behaviour of compacted silt used in a flood defence embankment in Indonesia. *Proceedings of the International Conference on Geotechnical and Highway Engineering*. Kuala Lumpur, Malaysia, 1-7.
18. Sun, D.A.; Sheng, D.C.; Cui, H.B.; and Li, J. (2006). Effect of density on the soil water-retention behaviour of compacted soil. *Proceedings of the Fourth International Conference on Unsaturated Soils*. Carefree, United States.
19. Tang, C.-S.; Cui, Y.-J.; Shi, B.; Tang, A.-M.; and Liu, C. (2011). Desiccation and cracking behaviour of clay layer from slurry state under wetting–drying cycles. *Geoderma*, 166(1), 111-118.
20. Laras, L.L. (2015). *Assessment to soil properties associated with desiccation crack of natural and metakaolin based geopolymer stabilized soil*. Dissertation, Institut Teknologi Sepuluh Nopember.
21. Yan, A.; Wu, K.; and Zhang, X. (2002). A quantitative study on the surface crack pattern of concrete with high content of streel fiber. *Cement and Concrete Research*, 32, 1371-1375.
22. Bezdek, J.C.; Hall, L.O.; and Clarke, L.P. (1993). Review of MR image segmentation using pattern recognition. *Medical Physics*, 20(4), 1033-1048.
23. Iyer, N.S.; Kandel, A.; and Schneider, M. (2000). Feature-based fuzzy classification for interpretation of mammograms. *Fuzzy Sets and Systems*, 114(2), 271-280.
24. Chuang, K.-S.; Tzeng, H.-L.; Chen, S.; Wu, J.; and Chen, T.-J. (2006). Fuzzy C-means clustering with spatial information for image segmentation. *Computerized Medical Imaging and Graphics*, 30(1), 9-15.
25. Pham, D.L.; Xu, C.; and Prince, J.L. (2000). Current methods in medical image segmentation. *Annual Review of Biomedical Engineering*, 2, 315-337.
26. Motorwala, A.; Shah, V.; Kammula, R.; Nannapaneni, P.; and Raijiwala, D.B. (2013). Alkali activated fly-ash based geopolymer concrete. *International Journal of Emerging Technology and Advanced Engineering*. 3(1), 159-166.

27. Joseph, D. (1994). Properties of geopolymer cements. *Geopolymer Institute*, 1-19.
28. Hardjito, D. (2005). *Studies of fly ash-based geopolymer concrete*. Doctoral thesis, Curtin University of Technology.
29. ASTM C618-19. (2019). *Standard specification for coal fly ash and raw or calcined natural pozzolan for use in concrete*. ASTM International, West Conshohocken, PA.
30. Palomo, A.; Grutzeck, M.W.; and Blanco, M.T. (1999). Alkali-activated fly ashes: a cement for the future. *Cement and Concrete Research*, 29(8), 1323-1329.
31. Davidovits, J. (1999). Chemistry of geopolymeric systems, Terminology. *Geopolymer '*99 *International Conference*, France.
32. Rangan, B.V. (2008). Low-Calcium fly-ash-based geopolymer concrete. Research report, Faculty of Engineering, Curtin University of Technology.
33. Hardjito, D.; Wallah, S.E.; Sumajouw, D.M.J.; and Rangan, B.V. (2004). On the development of fly ash-based geopolymer concrete. *ACI Materials Journal*, 467-472.
34. Alonso, S.; and Palomo, A. (2001). Alkaline activation of metakaolin and calcium hydroxide mixtures: influence of temperature, activator concentration and solids ratio. *Materials Letters*, 47(1-2), 55-62.
35. Sathia, R.; Babu, K.G.; and Santhanam, M. (2008). Durability study of low calcium fly ash geopolymer concrete. *Proceedings of the third ACF International Conference-ACF/VCA*. Ho Chi Minh, Vietnam, 1153-1159.
36. Swanepoel, J.C.; and Strydom, C.A. (2002). Utilisation of fly ash in a geopolymeric material. *Applied Geochemistry*, 17(8), 1143-1148.
37. Rattanasak, U.; and Chindaprasirt, P. (2009). Influence of NaOH solution on the synthesis of fly ash geopolymer. *Minerals Engineering*, 22, 1073-1078.
38. Sathonsaowaphak, A.; Chindaprasirt, P.; and Pimaraksa, K. (2009). Workability and strength of lignite bottom ash geopolymer mortar. *Journal of Hazardous Materials*, 168(1), 44-50.
39. Tang, C.; Shi, B.; Liu, C.; Zhao, L.; Wang, B. (2008). Influencing factors of geometrical structure of surface shrinkage cracks in clayey soils. *Engineering Geology*, 101(3-4), 204-217.
40. Gonzalez, R.C.; and Woods, R.E. (2002). *Digital image processing* (2nd ed.). Beijing: Publishing House of Electronics Industry.
41. Blum, H. (1967). *Models for the perception of speech and visual form*. Chapter: A transformation for extracting new descriptors of shape. Cambridge: MIT Press.
42. Fernández-Jiménez, A.; and Palomo, A. (2005). Composition and microstructure of alkali activated fly ash binder: effect of the activator. *Cement and Concrete Research*, 35(10), 1984-1992.
43. Rees, C.A.; Provis, J.L.; Lukey, G.C.; and Deventer, J.S.J. (2008). The mechanism of geopolymer gel formation investigated through seeded nucleation. *Colloids and Surfaces A*: *Physicochemical and Engineering Aspects*, 318(1-3), 97-105.
44. Widayanti, A.; Soemitro, R.A.A.; Ekaputri, J.J.; and Suprayitno, H. (2019). Tinjauan aspek ekonomi pemanfaatan reclaimed asphalt pavement dari jalan nasional di Provinsi Jawa Timur. *Jurnal Manajemen Aset Infrastruktur dan Fasilitas*, 3(2), 29-38.